

Extrinsic and intrinsic mechanisms directing epithelial cell sheet replacement during *Drosophila* metamorphosis

Nikolay Ninov, Dominic A. Chiarelli* and Enrique Martín-Blanco†

The fusion of epithelial sheets is an essential morphogenetic event. Here, we study the development of the abdomen of *Drosophila* as a model of bounded epithelia expansion and uncover a complex multistep process for the generation of the adult epidermis from histoblasts, founder cells that replace the larval cells during metamorphosis. We find that histoblasts experience a biphasic cell cycle and emit apical projections that direct their invasive planar intercalation in between larval cells. Coordinately, the larval cells extrude from the epithelia by apical constriction of an actomyosin ring and as a consequence die by apoptosis and are removed by circulating haemocytes. We demonstrate that the proliferation of histoblasts and the death of larval cells are triggered by two independent extrinsic Ecdysone hormonal pulses. Finally, we show that histoblast spreading and the death of larval cells depend on a mutual exchange of signals and are non-autonomous processes.

KEY WORDS: *Drosophila*, Metamorphosis, Histoblasts, Morphogenesis, Abdomen, Cell death, Cell replacement

INTRODUCTION

One of the main processes leading to the shaping of the three-dimensional body plan of higher organisms is the dynamic rearrangement of cell populations. Whereas in most morphogenetic processes cells move individually to new locations over large distances (i.e. during germ cell migration), in epithelia, during morphogenesis, cells reorganize themselves coordinately as a group (i.e. during neural tube folding).

The movement and fusion of epithelial cells during development is an essential and general morphogenetic event. Many different morphogenetic processes, both in vertebrates and invertebrates, and the related processes of adult and embryonic vertebrate wound healing, could be included in this category (reviewed by Martin and Wood, 2002). However, although extensive morphological descriptions of these processes represent classical paradigms of embryology, the genetic basis and the cellular behaviour underlying these events remain poorly understood. Thorough studies have shown that to undertake these processes epithelial cells can employ two alternative approaches: first, leading edge cells facing a free cellular space become specified and promote the migration of epithelial sheets acting as the main driving force for migration (in most cases in the absence of cell proliferation), e.g. *Caenorhabditis elegans* ventral enclosure (Williams-Masson et al., 1997) and imaginal discs fusion in *Drosophila* (Pastor-Pareja et al., 2004). Second, overall synchronous action of the whole epithelial cell population can induce global changes in its motility, conforming tissue shape changes, e.g. teleost epiboly (Trinkaus et al., 1992) and extension of the neural plate in *Xenopus* (Keller et al., 2000).

Two models of unbounded epithelial expansion, in which epithelial sheets with a free leading edge advance, meet and fuse to equivalent epithelial sheets in order to seal the surface of the animal, have been described in *Drosophila*. These models are dorsal closure and the fusion of imaginal discs. Dorsal closure is a late embryonic

event that begins with the elongation of the epidermal cells and finishes when the dorsalmost cells fuse at the midline (reviewed by Harden, 2002). The dimensions of the epidermal layer are not controlled by proliferation but are the result of changes in cell adhesion and cell shapes. Cells at the leading front that are planar polarized guide the migration of the epithelium, express specific markers and have a very active cytoskeleton. Dorsal closure depends on at least two signalling pathways – the JNK signal transduction pathway and the signalling pathway activated by Dpp (Martin-Blanco et al., 1998; Riesgo-Escovar and Hafen, 1997; Kockel et al., 1997). These two pathways are also involved in the expansion and merging of excorporated imaginal tissues (imaginal discs) at the expense of larval cells during metamorphosis (reviewed by Martin-Blanco and Knust, 2001). The imaginal discs evert and later on differentiate to give rise to the external structures of the adult. In this process the peripheral cells of the disc expand over the larval cells and gradually displace them. Finally, the discs recognize and fuse with each other to complete the continuous epithelium that will give rise to the head and the thorax of the adult.

Much less is known about the mechanisms controlling the movements of bounded epithelia without a free edge (e.g. the invagination of the basal region during sea urchin gastrulation, extension of the neural plate, rearrangement of scale precursors in the wings of insects, etc.) (see Bard, 1990). A potential model for the study of the coordinated expansion of this type of epithelia is the development of the adult abdomen of *Drosophila* during metamorphosis. The adult epidermis is formed by cells descending from histoblasts, founder imaginal cells specified during embryonic stages as small incorporated groups organized in nests. Each adult abdominal segment forms from four pairs of histoblast nests: the anterior and posterior dorsal pairs (which produce the tergites), the ventral pairs (which produce the sternites and pleurites) and the spiracular pairs (which form the spiracle and the surrounding pleurite tissues). Each anterior dorsal and ventral nest is composed of approximately 16 cells; each posterior dorsal nest consists of approximately five cells; and each spiracle nest has approximately three cells (Fig. 1A) (Guerra et al., 1973; Roseland and Schneiderman, 1979; Madhavan and Madhavan, 1980). During larval stages histoblasts are mitotically quiescent and arrested in G2 (Garcia-Bellido and Merriam, 1971; Madhavan and Schneiderman, 1977; Roseland and

Instituto de Biología Molecular de Barcelona, Consejo Superior de Investigaciones Científicas, Parc Científic de Barcelona, Josep Samitier 1-5, Barcelona 08028, Spain.

*Present address: Peter MacCallum Cancer Centre, 7 St Andrews pl, East Melbourne, Victoria, 3002, Australia

†Author for correspondence (e-mail: embbmc@cid.csic.es)

Schneiderman, 1979). At the onset of metamorphosis histoblasts undertake a rapid proliferation that allows them to expand and fuse, at the expense of the preexisting surrounding polyploid larval epidermal cells (LECs) that commit programmed cell death (Madhavan and Madhavan, 1980).

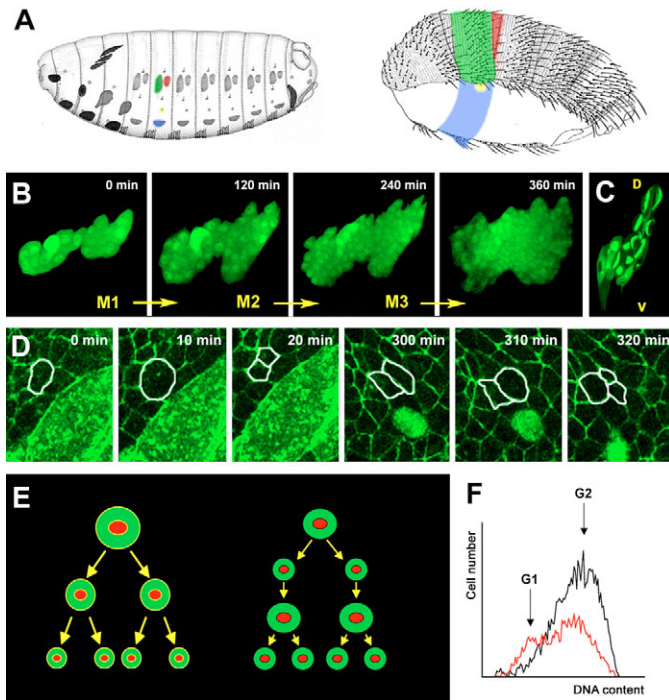


Fig. 1. Abdominal metamorphosis: cell proliferation dynamics of histoblasts. (A) During embryonic stages, four nests of abdominal histoblasts (adult epidermal cells precursors) can be distinguished in each hemisegment: anterior dorsal (green mask color), posterior dorsal (red), ventral (blue) and spiracular (yellow). During metamorphosis, histoblasts form the different structures that compose the abdominal adult epidermis, tergites (green), intersegmental membranes (red), pleurites and sternites (blue) and spiracle (yellow) (Roseland and Schneiderman, 1979). (B) In vivo time-lapse observation of histoblast proliferation in prepupal stages (1–6 hours APF) shows a synchronic cadence of three cell cycles leading to cell doubling every 2 hours. The number of cells calculated at the shown time points steadily increase (18, 36, 72 and 128). Cell sizes decrease after each mitosis (856, 605, 396 and 271 arbitrary 2-dimensional units; see Materials and methods). Histoblasts (anterior dorsal nest) expressed UAS-GFP under the control of Esg-Gal4 (see Movie 1 in the supplementary material). (C) Early histoblast cell divisions show planar orientation. Histoblasts (anterior dorsal nest) expressed UAS-Tau-GFP under the control of Esg-Gal4. In the first cell division, spindles orient predominantly along the dorsoventral axis. (D) Doubling times of histoblasts during pupal stages (from 15 hours APF onwards) increase up to 9 hours. Proliferation is stochastic and coupled to cell growth. Cellular outlines (anterior dorsal nest) were highlighted by ubiquitously expressing a DE-Cadherin-GFP fusion. Mitoses of individual cells were followed by in vivo time-lapse (see Movie 2 in the supplementary material). (E) Schematic of histoblast cell cycle dynamics. During prepupal stages (left), histoblasts do not grow between cycles (68% cell size decrease in the first three divisions). By contrast, during the pupal stages, histoblasts undergo intermitotic growth and their sizes remain constant (right). (F) FACS analysis showing cell cycle profiles of dissociated histoblasts from prepupal (black) and pupal stages (red). During prepupal stages, histoblasts lack or have a very reduced G1 phase. In pupal stages, the length of G1 phase increases by 70%.

Although the general characteristics of the expansion and fusion of histoblast nests are known from studies conducted 25 years ago, the molecular, genetic and cellular mechanisms involved in the generation of a functional epithelial barrier by histoblast are unknown. Furthermore, histoblasts represent an excellent model for in vivo studies at high resolution, as they constitute the external sheet of cells in the pupa and can be readily visualized across the pupal case. Our cellular characterization of the process has given light to numerous unanswered questions. What are the molecular mechanisms triggering abdominal epithelial morphogenesis? How do histoblasts achieve their migration within the epithelial layer? And how do LECs become removed in such a way that no gaps are formed in the epithelium during their massive cell death? We show that both proliferation of histoblasts and death of larval cells are triggered by extrinsic Ecdysone hormonal pulses occurring at different times during pupariation. Additionally, we have characterized the dynamics of the histoblast cell cycle and the cellular mechanisms underlying histoblast spreading and LEC death and removal. Finally, we have uncovered a potential intrinsic strategy for cell replacement directing the behaviour of histoblasts and LECs and its coordination.

MATERIALS AND METHODS

Fly stocks

All flies were maintained on standard culture media. Fly stocks used were as follows: Esg-Gal4 (*yw*; *NP5130*) (NIG-FLY Stock Center); Esg-Gal4 UAS-GFP (*y*, *w*; *NP5130*, *UAS-GFP*, *UAS-nGFP*, *UAS-lacZ/CyO*) (NIG-FLY Stock Center); Hs-FLP; Ay+Gal4 UAS-GFP (*hsp70-FLP*; *Act FRT y⁺ FRT Gal4*, *UAS-GFP/CyO*; *MKRSTM2*) (Ito et al., 1997); Esg-Gal4 Ay+Gal4 UAS-GFP UAS-FLP (*y*, *w*; *NP5130*, *Act FRT y⁺ FRT Gal4*, *UAS-GFP/CyO*; *UAS-FLP/TM6B*); Hs-Gal4 (*w*; *Hsp70 Gal4.PB 89-2-1*) (Bloomington Stock Center 1799); UAS-FLP (*y*, *w*; *UAS-FLP.Exel 3*) (Bloomington Stock Center 8209); 056-Gal4 – Enhancer trap ubiquitously expressed in the epidermis (*y*, *w*; *NP0056*) (NIG-FLY Stock Center); Ay+Gal4 UAS-GFP (*y*, *w*; *Act FRT y⁺ FRT Gal4*, *UAS-GFP*) (Bloomington Stock Center 4411); Srp-Gal4 UAS-GFP [*srpHemo-Gal4#16 A3B*, *UAS-Src-EGFP (II)*] (Bruckner et al., 2004); Sqh-GFP (*y w sqh^{AV3 cv}; sqh-GFP⁴²*) (Royou et al., 2004); UAS-*Rok^{CAT}* (Winter et al., 2001); UAS-P35 [*w*; *UAS-p35.H BHI (II)*] (Bloomington Stock Center 5072); UAS-Chickadee (L. Cooley, Yale University Medical School, Department of Genetics, New Haven, CT, USA); UAS-*MbsN300* (Lee and Treisman, 2004); UAS-Dap (*UAS-Dap II.3*) (Lane et al., 1996); UAS-EcR-RNAi (*UAS-EcR-AB RNAi*) (Schubiger et al., 2005); UAS-EcR^{DN} (*w*; *UAS-EcR.B1-DeltaC655.W650A*) (Bloomington Stock Center 6872); UAS-Rac^{V12} (*y*, *w*; *UAS-Rac1^{V12}*) (Bloomington Stock Center 6291); Stb-YFP (*w*; *Act Stb-YFP/TM3*) (Strutt et al., 2002); H2-YFP(III) [*His2avD-EYFP(II)*] (Rebollo et al., 2004); Hs-FLP Ay+Gal4 UAS-GFP H2YFP (*hsp70-flp*; *Act FRT y⁺ FRT Gal4*, *UAS-GFP/CyO*; *H2YFP/TM2*); Hs-FLP Ay+Gal4 UAS-GFP Stb-YFP (*hsp70-flp*; *Act FRT y⁺ FRT Gal4*, *UAS-GFP/CyO*; *Act Stb-YFP/TM2*); UAS-Src-GFP (*w*; *UAS-SrcEGFP M7E*) (Bloomington Stock Center 5432); UAS-Actin-GFP (*w*; *UAS-Act5C.GFP 2*) (Bloomington Stock Center 7310); DE-Cadherin-GFP [*Ubi-DE-Cad-GFP (II)*] (Oda and Tsukita, 2001); UAS-Tau-GFP (*w*; *UAS-GFP.tau*) (Brand, 1995).

Targeted expression in histoblasts

The Gal4/UAS system (Brand and Perrimon, 1993) was used for targeted expression in the histoblasts. The Esg-Gal4 was used as a histoblast-specific driver, although expression of this driver can also be detected in salivary glands, wing discs, eye discs and gut.

Permanent expression of UAS constructs in histoblasts

The Esg-Gal4 driver expression declines during late pupal stages. To overcome this problem we took advantage of the UAS-FLP/Actin-FRT-y+-FRT-Gal4 system (Struhl and Basler, 1993) by raising flies with the genotype *y*, *w*; *NP5130*, *Act FRT y⁺ FRT Gal4*, *UAS-GFP/CyO*; *UAS-FLP/TM6B*.

The larval expression of Esg-Gal4 triggers activation of the UAS-FLP transgene, which promotes the cis-recombination of FRT sites in the Actin-FRT-y⁺-FRT-Gal4 cassette generating a FLP-out event in histoblast cells. As a result, the Gal4 gene comes under the control of the Actin promoter, which promotes its permanent expression in histoblasts.

Time- and tissue-specific expression of UAS constructs in LECs

To achieve a tissue- and time-specific expression of UAS constructs in LECs we used a combination of the Gal4/UAS system and the FLP/FRT system by using the *hsp70-FLP*; *Act FRT y⁺ FRT Gal4, UAS-GFP/CyO*; *MRKS/TM2* strain (Ito et al., 1997). This system has been used for the generation of positively marked clones in diploid cells where the frequency of recombination is low (Struhl and Basler, 1993). The larval epidermal cells are polyploid and contain multiple copies of the genome. As a result the recombination frequency between FRT sites is far greater compared with diploid cells. A short heat shock treatment of 8-10 minutes leads to recombination, and hence the activation of a UAS-GFP reporter, in 95-100% of the larval epidermal cells 5-7 hours after the heat shock pulse. Heat shocks were performed during late larval stages (wandering larva) when histoblasts are mitotically arrested. In this way, we were able to express distinct UAS constructs in LECs although only small fractions of histoblast were affected (data not shown).

Immunohistochemistry

Primary antibodies used were: rabbit anti-laminin A antiserum at 1:100 dilution (Fessler et al., 1987), mouse anti-Fasciclin III (7G10-Hybridoma Bank) at 1:1000, mouse anti-GFP at 1:500 (Cell Signalling), rabbit anti-active Caspase 3 at 1:100 (Cell Signalling), mouse anti-EcRB1 at 1:10 (AD4.4 Hybridoma Bank) and mouse anti-EcRA at 1:10 (15G1A-Hybridoma Bank). Secondary antibodies were anti-mouse or anti-rabbit FITC, Cy3 or Cy5 conjugated (Molecular Probes) at 1:250 dilutions. Immunohistochemistry was performed using standard procedures. For pupal staging, white pupae [0 hours after puparium formation (APF)] were used as reference. After selection, the white puparium prepupa were transferred to fresh vials and kept at 25°C and standard humidity up to dissection. Whole pupae were bisected along the anteroposterior axis in sterilized 1× PBS (pH 7.4). The internal organs were cleaned from the epidermis by flushing with 1× PBS using a P10 pipette. The epidermis was detached from the pupal case using forceps and transferred to an ependorff tube on ice. Fixation was performed for 10 or 15 minutes in 4% paraformaldehyde. After fixation, the epidermis was rinsed three times in 1× PBS and permeabilized in sterilized PBT (0.3% Triton in 1× PBS) (3×15 minutes). After permeabilization, the tissue was blocked for 1 hour using PBTB [1% bovine serum albumin (BSA) in PBT]. Primary antibodies were incubated overnight at 4°C with gentle shaking. The epidermis was rinsed in 1× PBS, and washed 3×15 minutes in PBTB. After 1 hour blocking in PBTB, the secondary antibody was incubated for 3 hours at room temperature. After rinsing in 1× PBS, the tissue was stained using DAPI (1 ng/μl) to mark the nuclei and Rhodamine-coupled Phalloidin (Molecular Probes) at a dilution of 1:1000 from a 1 μg/μl stock solution was used to visualize polymerized actin. Finally the tissue was washed 3×15 minutes in 1× PBS, equilibrated in Vectashield (Vector) and mounted on coverslips. Actin staining using Phalloidin alone was performed as above after 10 minutes fixation and omitting the blocking steps.

In vivo imaging and time-lapse microscopy

Staged pupae and prepupae were washed in PBS. Early pupae were directly imaged through the transparent pupal case. For late pupal imaging (after 12 hours APF), a small window was opened into the pupal case on top of abdominal segments 2 and 3 by careful surgery with a fine needle. At this stage the pupal case is detached from the epidermis and can be removed without disturbing the underlying epidermis. The animals were positioned on a glass bottom microwell dish (MatTek) in a small drop of Voltaleff oil to improve optics and to avoid desiccation. Images were captured at different time intervals using an inverted Leica TCS 4D confocal microscope or an inverted Leica AOBs confocal microscope. Laser intensity was kept at a minimum to avoid photobleaching and to minimize phototoxicity. Each movie was repeated at least three times. In most cases, the animal survived the dissection and data acquisition and developed to adult stages.

In vivo quantification of cell proliferation rate

Cell proliferation was recorded using confocal time-lapse imaging in the posterior dorsal histoblast nest from 17 hours APF pupae of the genotypes *Hs-FLP*; *Ay+Gal4 UAS-GFP*; *H2-YFP* or *Hs-FLP*; *Ay+Gal4 UAS-GFP/UAS-P35*; *H2YFP/+*, where the expression of the P35 transgene was activated by heat shock during late larval stages. To minimize stress during image acquisition the pupal case was not removed and imaging was performed directly through the puparium at 10 minute intervals. Individual cells were followed from mitosis to mitosis using the ubiquitously expressed Histone2-YFP fusion protein as a marker. The mitosis of mother cells were taken as time 0 and the consecutive division of one of the two daughter cells as time 1. Cell doubling time was calculated for a time window of 6 hours (17-23 hours APF). Doubling times for 10 cells in each experiment were counted.

Flow cytometry

To measure the cell cycle phasing of the abdominal histoblasts, whole pupal cuticles (50 animals for each condition) were dissected, cleaned and then subjected to an incubation in 9× Tripsin, 1× PBS, with 1 mg/ml Hoechst 33342 for 3 hours at room temperature. Histoblasts were positively marked by Esg-Gal4 expression driving UAS-GFP. Prepupae animals were staged as less than 12 hours APF and greater than 3 hours APF. Early pupae animals were determined as greater than 12 hours APF and less than 24 hours APF. In order to compare cell cycle profiles, samples of each time point were prepared and ran simultaneously. We used a MoFlo flow cytometer (DakoCytometry, Fort Collins, Colorado, USA). Excitation was performed with an argon-ion laser of Coherent Enterprise II and the optical alignment obtained with fluorescent particles of a diameter of 10 μm (Flowcheck, Coulter Corporation, Miami, Florida, USA). Different populations were defined combining green (GFP) and blue (Hoechst 33342) emissions and the refringency parameters FSC and SSC.

Quantification of cell size

Cell size was calculated by dividing the number of cells in a histoblast nest over the total area of the nest. The area of the nest was calculated from z-stack projections covering the whole depth of the nest. Histoblasts were visualized using Esg-Gal4 driving the expression of a UAS-nuclear-GFP and UAS-cytoplasmic-GFP. Area measurements were carried out using ImageJ (NIH Image).

Image analysis

Image analysis was performed with Leica Confocal Software, Imaris 5D (Bitplane) software was used for 3D reconstruction of time-lapse movies, ImageJ (NIH Image) for cell tracking and mounting of time-lapse movies in AVI format, Photoshop 7.0 (Adobe Corporation) for data processing and Corel R.A.V.E. for conversion of movies to QuickTime format.

RESULTS

Histoblasts undergo biphasic dynamically controlled cell proliferation during metamorphosis

The abdominal histoblasts do not divide during the larval stages and increase in volume about 60-fold (Madhavan and Madhavan, 1980). Upon pupariation, histoblasts divide rapidly but remain confined to their original dimensions. A second, slower histoblast proliferation phase begins about 15 hours APF and lasts until about 36 hours APF. During this period, the histoblast nests enlarge, and the histoblasts replace the adjacent LECs. By time-lapse analysis, we validated these distinct phases. We found that during prepupal stages, histoblasts underwent very fast synchronous cell divisions, with a cell doubling time of around 2 hours (Fig. 1B; see Movie 1 in the supplementary material) and preferentially oriented spindles (Tau-GFP labelling, see Fig. 1C). This early stage lasted for three cycles and ran between 4 and 12 hours APF. A characteristic feature of the prepupal proliferation of histoblasts is the lack of cell growth between cycles, resulting in a rapid decrease in cell size (Madhavan and Madhavan, 1980) (Fig. 1E, left panel). We found by FACS

analysis that the short cell doubling time and lack of growth of histoblasts isolated at this stage was associated with a very reduced G1 phase (Fig. 1F).

During pupal stages, histoblasts enter a second phase of proliferation, in which synchrony gets lost and cell division planes become stochastically oriented. Our *in vivo* observations revealed a progressive increment of cell doubling times up to 9 hours (Fig. 1D; see Movie 2 in the supplementary material) resulting from a lengthening of 70% in the G1 phase (determined by FACS analysis) (Fig. 1F). As a result, histoblast cell size remained constant between mitosis (Fig. 1E, right panel). Combining these observations, we conclude that histoblast growth during the long quiescent larval period allows for the rather quick start to their differentiation, leading to a biphasic (quick and then slow) cell cycle profile.

Histoblast nest expansion requires the active planar intercalation of histoblasts into the larval epithelia

During the prepupal highly proliferative stage the area occupied by each histoblast nest did not significantly increase; as a consequence of this, as revealed by cytoskeleton (Actin) and adherens junction (DE-Cadherin) markers, histoblast nests became organized into pseudostratified monolayers (see Fig. S1A in the supplementary material). Subsequently, from 15 hours APF onwards, in synchrony with histoblast cell cycle slowness, nests initiated expansion and invaded the territories occupied by polyploid LECs. As an outcome, they rapidly rearranged into unstratified epithelia (see Fig. S1B in the supplementary material). The anterior and posterior dorsal nests fused into a single hemitergite nest between 15 and 18 hours APF (see Fig. S1C and Movie 2 in the supplementary material). Hemitergite nests from adjacent segments began to fuse at about 18 hours APF. The hemisternite (ventral) histoblast nest and the spiracular anlagen joined up between 18 and 22 hours APF, while the hemitergite histoblast nest and the spiracular anlagen joined up between 22 and 26 hours APF. The process was completed upon the fusion of left and right nests at the dorsal midline by 36 hours APF (Madhavan and Madhavan, 1980) (and data not shown).

To gain insight into the mechanisms involved in histoblast nest expansion, we monitored this process *in vivo*. This analysis revealed that at its onset, nest spreading proceeded through the intercalation of guiding histoblasts into the surrounding larval epidermal palisade (Fig. 2A; see Movie 3 in the supplementary material). To do so, invading peripheral histoblasts extended dynamic cellular protrusions in between neighbouring LECs that, by anchoring and shrivelling, promoted traction and the forward movement of histoblast cell bodies (Fig. 2B; see Movie 4 in the supplementary material). These structures were actin-rich and developed by effective actin polymerization at their tips, resembling actin comets (Fig. 2C,D; see Movie 5 in the supplementary material). The initial planar intercalation was followed by the coordinated expansion of the whole nest epithelia. Every cell at the edge of the nests weakly, but reproducibly, downregulated adherens junction markers (see Fig. S1C and Movie 2 in the supplementary material) and emitted both apical and basal filopodia and lamellipodia, which expanded over the surface of the LECs (Fig. 2E) and actively advanced over the underlying extracellular matrix (ECM) in the direction of migration (Fig. 2F). Nest expansion progressed centrifugally for several hours up to the merge of the adjacent ipsilateral and contralateral nests (data not shown). Finally, the sealing of the epithelia proceeded by the assembly of an apical purse string that brought together the apices of the leading cells (Fig. 2G; see Movie 6 in the supplementary material).

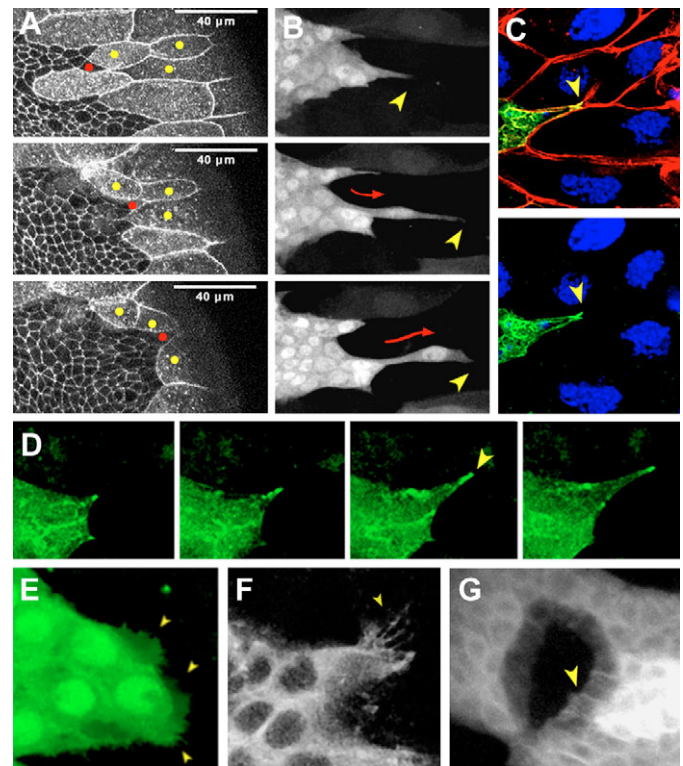


Fig. 2. The process of histoblast nest expansion is associated with cell shape changes and active cytoskeleton dynamics.

(A) Snapshots of the process of histoblast expansion (ubiquitous DE-Cadherin-GFP; see Movie 3 in the supplementary material) show that at early stages of nest spreading (anterior dorsal nest), leading cells intercalate within and disjoin LECs. A leading histoblast (red) successively intercalates in between individual LECs (yellow). Overall, leading histoblasts move over a distance of 40 μm in 3 hours. (B) Leading histoblasts (Esg-Gal4/UAS-GFP, posterior dorsal nest) extend invasive dynamic protrusions (arrowheads), which promote the forward movement of histoblast cell bodies (red arrows) (see Movie 4 in the supplementary material). (C) The long cellular protrusions of histoblasts are enriched with actin at their tips (arrowheads). UAS-Actin-GFP was expressed in histoblasts (Esg-Gal4) and visualized with anti-GFP antibodies (green). Cell morphology was revealed by Phalloidin staining. Nuclei are in blue (DAPI). (D) The protruding structures of leading histoblasts grow by distal actin filament polymerization (arrowhead). Actin dynamics *in vivo* were monitored with Actin-GFP (Esg-Gal4) by confocal time-lapse microscopy (anterior dorsal nest) (see Movie 5 in the supplementary material). (E) Spreading histoblasts (Esg-Gal4/UAS-GFP, posterior dorsal nest) crawl over the larval epithelia and send out apical cellular projections in the form of lamellipodia and small filopodia (arrowheads). (F) Long filopodia (arrowhead) are observed in the basolateral membrane of peripheral histoblasts (Esg-Gal4/UAS-GFP, anterior dorsal nest). These structures are enriched in filamentous actin and are highly motile. (G) During the fusion of neighbouring histoblast nests, the apical domains of adjacent histoblasts become organized in a purse string (arrowhead). Histoblasts (Esg-Gal4/UAS-Src-GFP, spiracular and ventral nest) were monitored by time-lapse confocal microscopy (see Movie 6 in the supplementary material).

Altogether, these results reveal a complex, multistep process that involves the invasion of the larval epithelia by histoblasts (planar intercalation) mediated by active cellular actin-rich protrusions. To test this model we interfered with actin polymerization in histoblasts. During *Drosophila* bristle morphogenesis, the activities of the products of the *cpb* (Capping protein beta) and *chickadee* (Profilin)

genes hold a tight balance between actin depolymerization and assembly (Hopmann and Miller, 2003). Loss of Cpb or excessive Profilin activity resulted in actin accumulations and abnormal bristles. In this light, we overexpressed Profilin in histoblasts under the control of a permanent Esg-Gal4 driver (see Materials and methods). The overexpression of Profilin disrupted bristle morphogenesis, as expected, and caused the inefficient expansion of histoblast nests, provoking abdominal clefts (Fig. 3A). In this condition, actin aggregated within histoblasts (compare Fig. 3B with 3C) and, in contrast to wild-type nests, where numerous long protrusions formed during expansion, Profilin-overexpressing histoblasts lacked such structures and just exhibited rare short filopodia and lamellipodia (Fig. 3D; see Movie 7 in the supplementary material). Moreover, the transition of histoblast nests from pseudostratified epithelia to an unstratified monolayer was delayed (data not shown). Thus, the inability of histoblasts to resort to long cellular protrusions resulted in the delay of their expansion and migration, suggesting that the actin-mediated planar intercalation of histoblasts between LECs is essential for their proper expansion.

The replacement of LECs relies on their basal extrusion, which is mediated by myosin contractility and is independent of haemocyte recruitment

The expansion of histoblast nests is directly coupled to the replacement of the LECs, as no gaps in the epidermis are ever detected histologically. But, how is cell replacement achieved? By time-lapse analysis we found that simultaneously with nest expansion, LECs collapsed, were extruded and died under the epithelial layer (Fig. 4A,B; see Movie 8 in the supplementary material).

What is the mechanism for basal extrusion of LECs? Are the histoblasts pushing away the polyploid LECs (Fig. 2B)? Or are pulling contractile forces from the LECs driving nest expansion? Or a combination of both? To analyse these issues we evaluated actomyosin dynamics during the expansion of histoblast nests. Myosin II regulatory light chain (Spaghetti squash) (Royou et al.,

2004) accumulated as perimetral rings in the apical domain of LECs. Assessment of video time-lapse recordings revealed that LEC extrusion was initiated by apical constriction, apparently mediated by actomyosin contraction (Fig. 4C; see Movie 9 in the supplementary material). The apical constriction of LECs seemed to be a cell-autonomous event, as it could be observed occasionally in LECs without direct contact with the expanding histoblasts but several cell diameters away.

Non-muscle myosin II is a hexamer composed of two of each of three subunits: the heavy chain, the regulatory light chain (MRLC) and the essential light chain (Korn and Hammer, 1988). The force-generating activity of actomyosin is mainly controlled through the phosphorylation of the MRLC (Craig et al., 1983). Two kinases, Rho-kinase (Rok; also known as Rock) (Winter et al., 2001) and Myosin light chain kinase (MLCK) (Totsukawa et al., 2000) phosphorylate MRLC in both mammals and *Drosophila* and activate myosin contraction. By contrast, dephosphorylation of MRLC by myosin light chain phosphatase (MLCP) inhibits myosin activity. This serine/threonine protein phosphatase is a heterotrimer consisting of a catalytic subunit, a 20 kDa protein of unknown function, and the myosin binding subunit (MBS) that targets MLCP to MRLC (Fukata et al., 1998). Phosphorylation by Rok of a specific threonine within a conserved motif in MBS has been shown to inhibit MLCP activity, suggesting that Rok activates MRLC both by direct phosphorylation and also by inhibition of MBS (Kawano et al., 1999).

To test whether myosin contraction was required for cell delamination, we overexpressed in LECs a truncated constitutively active form of the *Drosophila* MBS orthologue (MbsN300) that cannot be phosphorylated by Rok (generalized clonal expression of UAS-MbsN300; see Materials and methods) and inhibits Myosin contractility (Lee and Treisman, 2004). In this condition, a significant proportion of LECs did not extrude and remained within the abdominal epidermis at postmetamorphosis periods (Fig. 4D). As a consequence, cuticular clefts were observed in the abdomen (Fig. 4E). Further, we found that the overexpression of a constitutively active form of Rok (Rok^{CAT}) (Winter et al., 2001), which upregulates myosin contractility, led to premature

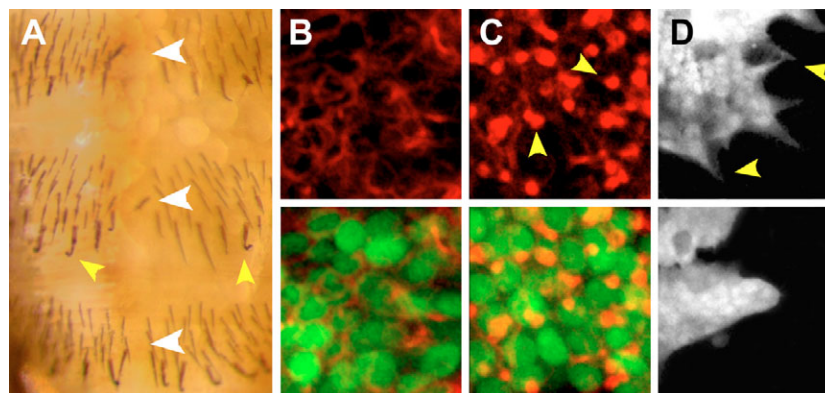


Fig. 3. Actin polymerization directs the expansion of histoblast nests. (A) Bristles with morphogenetic defects (yellow arrowheads) and cuticular abdominal clefts (white arrowheads) in an adult escaper of Permanent-Esg-Gal4/UAS-Profilin genotype. (B) In wild-type histoblasts (22 hours APF), most polymerized actin organizes in cortical filaments. Phalloidin-rhodamine staining (red) is shown in the top and bottom panels. UAS-GFP expression (green) under the control of Permanent-Esg-Gal4 is shown in the bottom panel. (C) Actin in histoblasts overexpressing Profilin (22 hours APF) hyperpolymerizes and accumulates in intracellular clumps (arrowheads). Top and bottom panels are as in B. (D) Snapshots from Movie 7 in the supplementary material. Top panel, wild-type dorsal posterior nest (23 hours APF). Arrowheads point to expanding peripheral protrusions. Bottom panel, dorsal posterior nests from pupae (23 hours APF) overexpressing Profilin (Permanent-Esg-Gal4/UAS-GFP; UAS-Profilin). Note the absence of long terminal protrusions and the histoblast expansion delay.

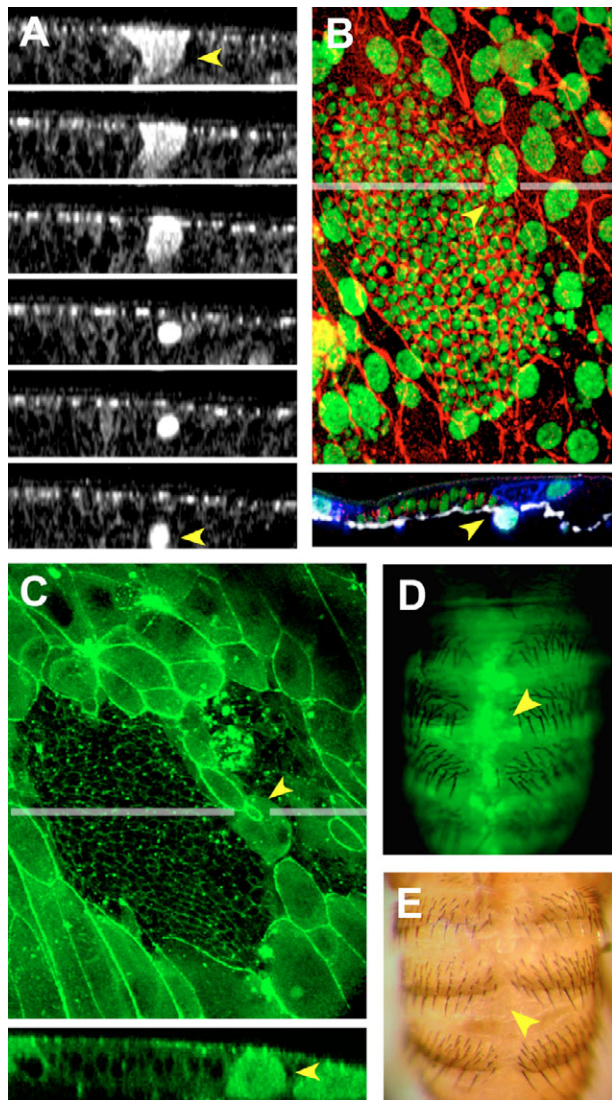


Fig. 4. LECs are basally extruded during histoblast nest expansion by a mechanism involving the assembly of an actomyosin apical contractile ring. (A) Transverse snapshots (z-axis) of a 4D confocal reconstruction show the progression of the delamination of an intervening LEC (arrowhead) between the anterior and the posterior dorsal nests. Cells were marked using DE-Cadherin-GFP and the fusion of histoblast nests was monitored by time-lapse confocal microscopy (see Movie 8 in the supplementary material). (B) DAPI staining (green) shows that LECs in the epithelial layer (adjacent to the ventral histoblast nest) have large polyploid nuclei that become condensed (arrowhead) upon extrusion. Apical compartment outlines were visualized using a Fasciclin III antibody (red). A transverse section (lower panel) shows an extruded LEC surrounded by the ECM (arrowhead). The basal lamina was labeled by laminin A (white) and LEC (056-Gal4) membranes were marked using a UAS-*Src*-GFP (false blue colour). (C) The actomyosin cytoskeleton of histoblasts and LECs was visualized by a myosin light chain GFP fusion protein (*Sqh*-GFP) under the control of its own promoter (green). *Sqh*-GFP is present in apical LEC membranes. LECs initiating basal extrusion between the anterior and the posterior dorsal nests (see Movie 9 in the supplementary material) show apical myosin constriction (arrowhead and transverse optical sections, lower panel). (D) Persistent LECs (arrowhead) in a pharate adult clonally expressing GFP (green) and MBSN300, which leads to the constitutive dephosphorylation of MRLC and the inhibition of Myosin contractility. (E) Cuticular abdominal clefts (arrowhead) in an adult escaper clonally expressing MBSN300.

delamination of LECs. In wild-type animals, LECs extrude progressively at a very stereotyped speed. Thus, out of 70 ± 2 LECs found in the dorsal posterior compartment of abdominal segments in third instar larvae, only 14 ± 2 cells remained in place at 24 hours APF. The targeted overexpression of *Rok*^{CAT} in these cells (*En-Gal4/UAS-Rok*^{CAT}) accelerated their delamination and, in the same period and starting from the same number of original cells, only three to five remained within the epidermal layer. Altogether, these results strongly suggest that the apical constriction of LECs plays a significant role at the initiation of the cell replacement process and that apical actomyosin contractility is both necessary and sufficient for the extrusion of LECs.

Clearance of apoptotic corpses by macrophages seems to have major consequences in many developmental processes (Sears et al., 2003). In *Drosophila*, the phagocytic function is performed by circulating haemocytes (Tepass et al., 1994), and we found that *Serpent*-expressing haemocytes densely populated the basal lamina of the abdominal epidermis (Fig. 5A). Is the actomyosin-driven apical contraction the only significant activity resulting in the rapid elimination of LECs? Close examination of the process of replacement revealed that, during their apical constriction, LECs became surrounded on their basal side by bright fluorescent motile bodies, which we identified as haemocytes (Fig. 5B). Double-labelling video time-lapse using *Srp*-Gal4 driving GFP expression in haemocytes and a *Stb*-YFP apical membrane epithelial marker ubiquitously expressed showed that the extrusion of LECs was a coordinated process in which apical constriction was immediately followed by encapsulation from the basolateral surface by haemocytes (Fig. 5C; see Movie 10 in the supplementary material). No cell blebbing was observed before extrusion, but LEC nuclei collapsed and then became fragmented upon engulfment, turning TUNEL-positive (data not shown). Is thus corpse removal by haemocytes required for the expansion of histoblast nests and abdominal morphogenesis? To assess this issue we genetically blocked the migratory capacity of haemocytes by expressing a constitutively active form of the small GTPase *Rac* (*Rac*^{V12}) (Paladi and Tepass, 2004). The expression of *Rac*^{V12} under the *Srp*-Gal4 driver resulted in a 100% penetrant absence of *Srp*-Gal4/UAS-GFP-expressing haemocytes from the abdomen at 24 hours APF (data not shown). The inability of haemocytes to migrate into the abdomen generated late pupal lethality; nonetheless, the morphogenesis of the adult abdomen proceeded relatively normally (data not shown). Overexpression of *Ricin* or a dominant-negative form of *Pvr*, which is necessary for haemocyte survival, led to similar phenotypes, albeit not 100% penetrant. These results suggest that haemocytes are dispensable for the expansion of the histoblast nests at the expense of LECs.

Ecdysone signalling is required for both the proliferation of histoblasts and the death of LECs

The larval-prepupal transition of *Drosophila* is associated with a peak of ecdysteroids that terminates larval feeding, initiates premetamorphic behaviours and commits larval tissues to a pupal fate. A second Ecdysone pulse, approximately 12 hours APF, defining the prepupal-to-pupal transition, follows this larval peak (Riddiford, 1993). In *Drosophila*, the response of tissues to Ecdysone is mediated by a heterodimer of the Ecdysone receptor (*EcR*) and *Usp*, both nuclear receptor proteins (Koelle et al., 1991; Yao et al., 1992). Ecdysone receptors directly induce the transcription of primary-response genes. Some of these early genes encode transcription factors that regulate large batteries of secondary-response late genes (reviewed by Thummel, 2001). The

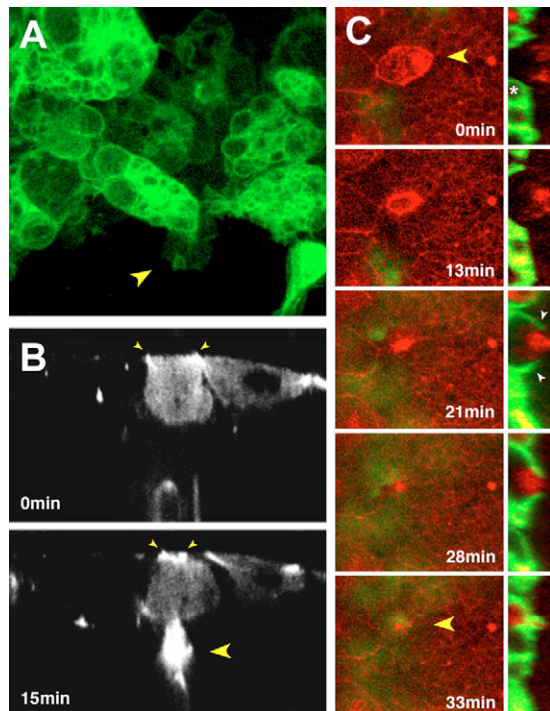


Fig. 5. Extruded LECs are removed by circulating haemocytes. (A) Macrophage-like haemocytes circulate under the pupal epidermis basal lamina extending and retracting leading lamellipodia (arrowhead). Haemocytes were visualized *in vivo* through the pupal cuticle by the expression of membrane-bound Src-GFP (green) using a haemocyte-specific driver (*Srp-Gal4*). (B) Travelling cells in the haemolymph are recruited to the basal surface of LECs. The actomyosin cytoskeleton of LECs was visualized by the expression of *Sqh-GFP* using confocal XZT acquisition. The apical constriction of LECs (small arrowheads) was followed by the attachment of bright fluorescent bodies to their basal side (large arrowhead). (C) The recruitment of haemocytes to the basolateral surface of LECs occurs sequentially to constriction. Simultaneous *in vivo* visualization of LECs and histoblasts (ubiquitous expression of *Stb-YFP*, red) and haemocytes (*Srp-Gal4/UAS-GFP*, green) (see Movie 10 in the supplementary material). Snapshots show LECs undergoing apical constriction (arrowhead) and being engulfed from their basal surface by haemocytes (asterisk) extending cytoplasmic projections (small arrowheads). Transverse z-projections show that encapsulation initiates before LEC delamination is completed and is extremely fast. The whole process (apical constriction, delamination and engulfment) takes place in approximately 45 minutes.

EcR gene encodes three isoforms: *EcR-A*, *EcR-B1* and *EcR-B2*, which share common DNA- and ligand-binding domains but differ in their N-terminal sequences. During larval stages, imaginal discs express high levels of *EcR-A*, whereas most larval tissues and the imaginal histoblasts predominantly express *EcR-B1* (Talbot et al., 1993). This pattern changes upon pupariation, and histoblasts and LECs then express both *EcR-A* and *EcR-B1* isoforms (see Fig. S2 in the supplementary material).

Two divergent developmental programmes appear to be activated by Ecdysone during metamorphosis: the massive destruction of obsolete larval tissues (salivary glands, midgut and fat body) and the simultaneous differentiation of adult tissues (imaginal cells). To investigate whether Ecdysone is responsible for triggering abdominal morphogenesis, we expressed an RNAi construct (Schubiger et al.,

2005) or a truncated version of its receptor (Cherbas et al., 2003) either in histoblasts (*Esg-Gal4*) or in the LECs at the onset of metamorphosis. Contrary to published reports (Bender et al., 1997), blocking autonomously Ecdysone signalling in histoblasts completely abolished their proliferation up to the time of nest spreading (Fig. 6A), when cell division resumes. This yielded viable adults with variable abdominal defects (data not shown). We interpret this variability as being a consequence of the decay of the *Esg-Gal4* driver expression (data not shown), which might fail to sustain *EcR* inhibition. Conversely, clonal autonomous expression of a truncated (dominant-negative) form of *EcR* in LECs completely blocked their ability to apically constrict, extrude and undergo apoptosis. As a result, abdominal morphogenesis did not succeed, and LECs were still present in the abdomen of pharate adult flies, forming part of the epidermis (Fig. 6B). We conclude that Ecdysone signalling triggers the onset of proliferation in the histoblasts upon pupariation and primes the death of the larval cells in coordination with histoblast nest spreading.

Coordination of proliferation and cell death

During the early stages of histoblast proliferation, cell division takes place in the absence of cell growth. By contrast, during late stages, histoblasts couple proliferation with growth. Interestingly, the shift in the histoblast cell cycle precedes the onset of LEC death, suggesting that histoblast growth might influence non-autonomously the triggering of LEC apoptosis.

To explore whether cell growth and cell death during cell sheet replacement are coordinated and interdependent processes, we performed two types of analysis. First, we blocked the proliferation of histoblasts and monitored the non-autonomous effects on LECs. Strong inhibition of proliferation by interfering with Ecdysone signal reception (see above) or by permanent overexpression of *Dacapo*, an inhibitor of Cyclin E-Cdk2 (*Cdc2c* – FlyBase) complexes and G1 to S progression (de Nooij et al., 1996), in histoblasts (Fig. 7A) resulted in a profound delay in LEC death (Fig. 7D,E). In none of these cases was the developmental timing of pupariation and unrelated processes, such as head and imaginal disc eversion, affected (data not shown). Pharate adults escapers showed multiple differentiation and morphogenetic abdominal defects (data not shown).

In addition, we prevented the death of LECs by interfering in the caspase cascade. The clonal expression of the apoptosis inhibitor *P35* in LECs (see Materials and methods) resulted in LEC survival, impaired extrusion due to the partial inhibition of LEC apical constriction (Fig. 7B) and failure in the recruitment of haemocytes and the engulfment process. Those few LECs able to undergo extrusion in the presence of *P35* remained viable cells (as judged by their nuclear and cellular morphology) under the epithelial layer (Fig. 7C).

In this condition, we found a significant decrease in the progression of histoblast nest spreading and the average number of histoblasts (Fig. 7F). These non-autonomous effects were a consequence of the delamination and death of numerous histoblasts (Fig. 7G), which does not occur in wild-type animals (data not shown). Histoblast death compensates and surpasses a weak non-autonomous enhancement of their mitotic index (Fig. 7H). Pharate adults could be recovered, but they showed abdominal cuticle clefts with many LECs still present (data not shown). These results strongly support a mechanism coordinating proliferation and spreading of histoblasts with the programmed death of LECs. Whether this mechanism relies on mutual signalling events, mechanical forces or cell competition for survival factors remains to be determined.

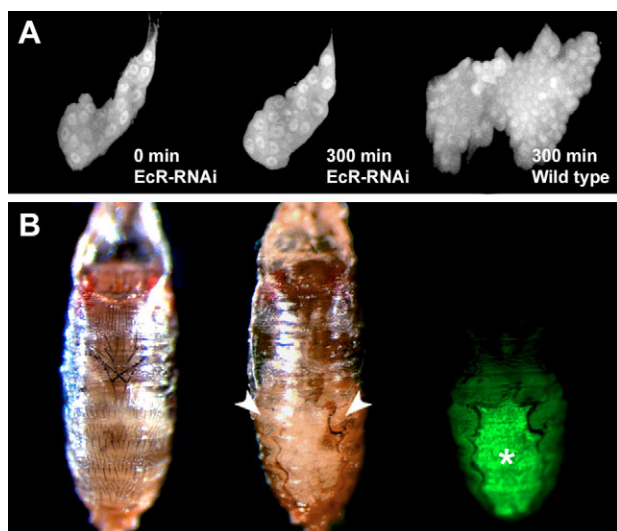


Fig. 6. Histoblast proliferation and LEC death are triggered by Ecdysone signaling. (A) Blocking Ecdysone signaling autonomously in histoblasts abolished their proliferation. The overexpression of an Ecdysone receptor EcR-RNAi construct (Esg-Gal4) results in a prolonged delay in cell division. The left image shows a dorsal anterior nest at the prepupal stage expressing EcR-RNAi. The number of histoblasts in this nest is similar to equivalent nests in wild-type pupae (see Fig. 1B). The middle image shows the same nest 300 minutes later; histoblasts have not divided. In this period, wild-type animals undergo three rounds of division (right image). (B) Clonal autonomous inhibition of Ecdysone signalling in LECs (dominant-negative form of the Ecdysone receptor EcR-DN) blocks their death (see Materials and methods). The left image shows a control animal in which the abdominal epithelial fusion proceeds normally. As a result of the overexpression of EcR-DN (middle image) the expansion of histoblast nests does not succeed, resulting in a dorsal scar phenotype (arrowheads). Simultaneous expression of a GFP marker reveals that LECs (asterisk) have not been eliminated from the abdomen of pharate adult mutant flies (green: right image).

DISCUSSION

Hormonal control of abdominal morphogenesis

Ecdysone acts as a significant temporal signal in *Drosophila*, triggering each of the major developmental transitions. Although we know most of the genetic elements involved in Ecdysone signal transmission (Thummel, 2002), the difficulty in visualizing morphogenetic changes in vivo and interfering with signal reception in individual cells has become a major impediment in our understanding of Ecdysone actions during metamorphosis.

In vitro culture studies have shown that Ecdysone pulses are crucial for the morphogenesis of adult appendages (Milner, 1977). Other studies have uncovered the ecdysteroid dependence of multiple differentiative and maturational responses (Schubiger et al., 1998). Nonetheless, little is known about ecdysteroid control of cell proliferation. A revealing analysis in *Manduca* showed that proliferating cells of the optic lobe reversibly arrest in G2 whenever the concentration of ecdysteroid drops below a critical threshold (Champlin and Truman, 1998). Furthermore, earlier studies had shown that the number of histoblasts is reduced in hypomorph mutants for EcR isoforms (Bender et al., 1997). Whether this was the result of lack of proliferation or cell death had not been defined. Here, we show in vivo a direct role for Ecdysone in cell proliferation (see Fig. 8). The rapid cell cycles experienced by abdominal

histoblasts at the end of the third larval instar halt if Ecdysone-signalling reception is cell-autonomously compromised (Fig. 6A). Histoblasts remain quiescent in G2 and competent to resume proliferation in response to late Ecdysone pulses. Our observations suggest that Ecdysone signalling controls the cell cycle by regulating the expression of genes involved in the G2-to-M transition (N.N., M. Grande and E.M.-B., unpublished).

The destruction of larval tissues in *Drosophila* also results from a major transcriptional switch triggered by Ecdysone. The anterior larval muscles and larval midgut (Lee et al., 2002) and the head and thoracic LECs (N.N. and E.M.-B., unpublished) degenerate during the first half of prepupal development (prepupal Ecdysone peak), while the larval salivary glands (Jiang et al., 2000), abdominal muscles and abdominal LECs (see Fig. 5) histolyze after the second Ecdysone pulse (pupation). Given that the exposure to Ecdysone is systemic, the stage-specific cell death responses of different cell types to Ecdysone must be differentially regulated.

The death of abdominal LECs shows apoptotic characters and proceeds in two steps: the basal extrusion of cells initiated by the contraction of an apical actomyosin ring, and their removal by haemocytes (see Figs 5, 6 and 7). The cell-autonomous inhibition of EcR activity in LECs led to abortive extrusion and cell survival (Fig. 6B). Thus, the death of LECs share with other obsolete larval cells a common priming hormonal (Ecdysone) input (Fig. 8).

It is still not clear how cell proliferation and cell death are differentially controlled by Ecdysone. The trigger of histoblast proliferation seems to be directly dependent on Ecdysone signalling. However, we still do not know how the onset of LEC death is set. In other words, how do LECs distinguish between the late larval and the pupal Ecdysone pulses? In a plausible scenario, to avoid detrimental epithelial gaps at the surface, signalling clues from 'matured' histoblasts (after their rapid proliferation in response to the initial prepupal Ecdysone pulse), could assist Ecdysone signalling to instruct LECs to die. Indeed, LECs do not die in response to the pupal Ecdysone pulse if histoblast proliferation (and hence, 'maturation') has been experimentally delayed (Fig. 7). The identification and characterization of this putative signal awaits further genetic and molecular analysis. Thus, Ecdysone signalling is necessary, but not sufficient, for LEC death.

The control of the cell cycle

The developmental control of cell cycle dynamics and diversity represents a key regulatory mechanism that directs cell size, cell number and ultimately the organ size of adult individuals. Despite numerous elegant experiments, the details of how cell division is regulated and coupled to cell growth remain poorly understood.

During abdominal morphogenesis, the trigger of cell proliferation occurs simultaneously in all histoblast nests within each segment. Cell counting reveals that up to eight cell divisions are required to build the complete adult hemitergite (Merriam, 1978). The same proportions apply to the ventral and spiracular nest. We have found that the first three histoblast divisions during pupariation are synchronous and extremely fast, skip the G1 phase and resemble the early embryonic blastoderm divisions (Fig. 1). In this early stage, histoblast cleave and progressively reduce their size. We found that Ecdysone signalling is involved in the initiation of the proliferation programme (see above). But, how is the histoblast cell cycle regulated to achieve fast proliferation in the absence of cell growth? Does it rely on the storage of preexistent control molecules, as in early embryos (Knoblich et al., 1994), or is it linked to signals impeding their growth? While this issue remains to be unravelled, the extreme growth of histoblasts during previous larval stages

Fig. 7. The proliferation of histoblasts and the death of LECs are coordinated by reciprocal interactions.

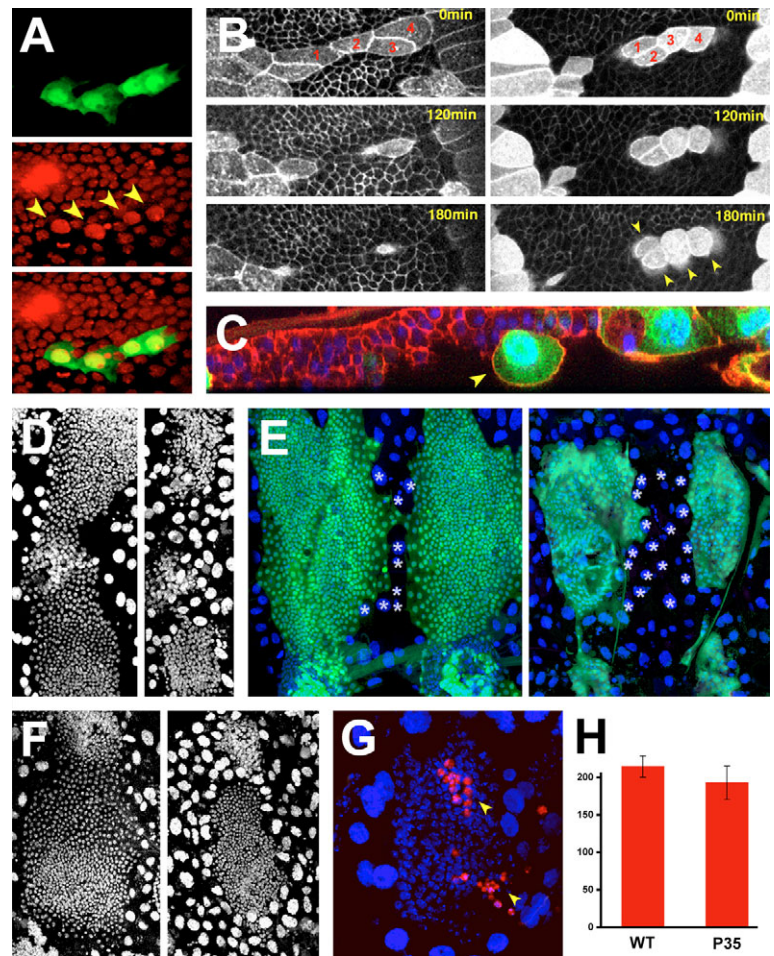
(A) Histoblast early divisions are autonomously blocked by Dacapo. UAS-Dacapo overexpressing clones labelled with GFP (green) were generated using FRT recombination.

Dacapo-expressing histoblasts (arrowheads) in the anterior dorsal nest become arrested after two cell cycles and remain enlarged in comparison with wild-type neighbours. Nuclei were labelled by the expression of Histone H2-YFP (red). (B) LECs expressing P35 (induced by FRT recombination-GFP expressing cells) showed impaired cell extrusion due to partial inhibition of their apical constriction. The delamination of LECs expressing P35 (right panel) is strongly delayed and LECs persist in the epithelia for at least 3 hours longer than their wild-type counterparts (arrowheads). Larval cells and histoblasts were labelled using a DE-Cadherin-GFP fusion (wild type) and Stb-YFP, an apical membrane marker.

(C) Those few LECs able to undergo extrusion in the presence of P35 remained as viable cells under the epithelial layer (as judged by their nuclear and cellular morphology) and were not engulfed by haemocytes. Cell outlines were visualized using Phalloidin (red) and cell nuclei were labelled with DAPI (blue). Note that the histoblast layer becomes highly pseudo-stratified. (D) The overexpression of Dacapo by heat shock results in the inhibition of cell division in all pupal cells, smaller histoblast nest sizes (DAPI staining) and in the survival of LECs, which remained in the epithelia. Staged heat shocked (right panel) and wild-type (left panel) pupae were dissected at 25 hours APF. Thus, the decreased proliferation rate of histoblasts correlated with a strong reduction in LEC death rate.

(E) To exclude indirect anti-apoptotic effects of Dacapo in LECs (see B), Dacapo was exclusively and permanently expressed in histoblasts (see Materials and methods). In this condition (right panel), histoblast nests (green) are smaller than wild-type ones, with fewer cells (left panel) (25 hours APF). LECs (which do not express Dacapo) are not eliminated from the epithelia (asterisks). Thus, the reduction of LEC death rate caused by inhibition of histoblast proliferation is non-autonomous.

(F) The delayed elimination of LECs expressing P35 causes a non-autonomous decrease in the number of histoblasts. The average reduction in histoblast numbers (DAPI staining) from ventral nests of animals subjected to FRT recombination (right panel) in comparison with wild-type animals (left panel) at 24 hours APF was approximately 20%. (G) The primary cause of the non-autonomous reduction in histoblast numbers is cell death. P35 expression in LECs (ventral nest, 24 hours APF) results in significant ectopic non-autonomous delamination and death (arrowheads) of histoblasts. Apoptosis was monitored by activated Caspase-3 antibody staining (red). (H) Inhibition of LEC death by P35 does not result in a major change in doubling times for histoblast. Quantification of cell division rates in posterior dorsal nests was performed by time-lapse analysis (from 17 hours APF) and cell counting (see Materials and methods). Cell doubling times are shown in minutes.



makes plausible the accumulation of G1 regulators, which, upon Ecdysone signalling, could allow a fast transition through G1 phase. Indeed, we have found that Cyclin E concentration (which regulates entry into S phase) in histoblasts builds up during the larval period. The observed deceleration of histoblast proliferation could then be the consequence of the exhaustion of the entire stock of Cyclin E (N.N., M. Grande and E.M.-B., unpublished). Still, the implication of growth control mechanisms in the regulation of histoblast proliferation cannot be ruled out. Multiple cell types, such as the animal-cap blastomeres from *Xenopus* embryos (Wang et al., 2000), change their cell cycles from size-independent to size-dependent after they become smaller than a critical cell size. Histoblasts might sense size in an analogous way. Thus, pathways that regulate growth, such as insulin-mediated signalling, Myc and Ras oncoproteins and the products of the Tuberous sclerosis complex 1 and 2 genes (reviewed by Jorgensen and Tyers, 2004), should be explored to evaluate their potential roles in the coupling mechanism linking growth and cell cycle progression.

The mechanism of histoblast spreading

Histoblast nest spreading initiates with the projection of leading comet-like protrusions, followed by apical cytoskeletal activity and active crawling over the underlying basal membrane, and terminates with the implementation of an apparent purse string, reminiscent of those described during dorsal closure, *C. elegans* ventral enclosure or wound healing (reviewed by Martin-Blanco and Knust, 2001).

The comet-like protrusions of guiding histoblasts break through the LEC epithelial barrier, leading to planar intercalation of histoblast cell bodies (Fig. 2; see Movie 4 in the supplementary material). They account for the capacity of histoblasts to achieve migration within the bounded epithelial layer. Indeed, electron micrographs reveal that the advancing histoblasts form junctions with non-adjacent LECs before the adjacent LECs histolyze, thus insuring the continuity of the epidermis (Roseland and Reinhardt, 1982). Time-lapse observations (see Movie 5 in the supplementary material) suggest that these protrusions grow by sequential addition of actin molecules at their forward end (see Bershadsky, 2004). In this sense, they resemble,

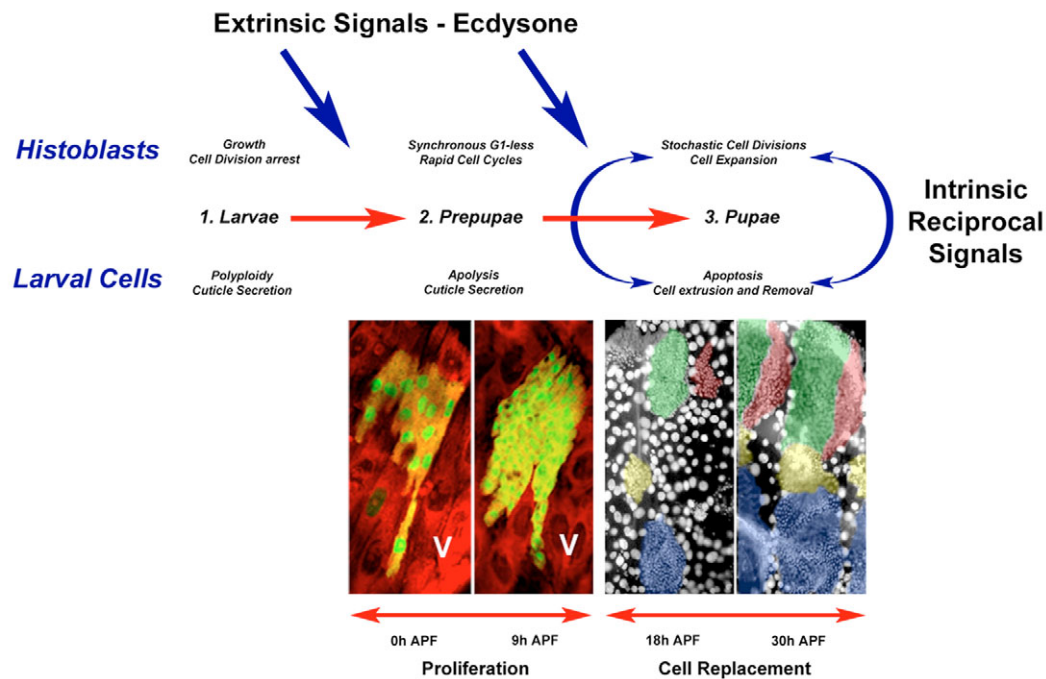


Fig. 8. Extrinsic and intrinsic signals on the process of generating an epithelial sheet de novo: LEC replacement by histoblasts. During larval stages, histoblasts are arrested in G2 and increase their size. LECs endoreduplicate, become polyploid and secrete the larval cuticle. At the onset of metamorphosis, the histoblasts undergo a series of G1-less synchronous cell divisions and reduce their size. Histoblast nests do not expand and remain confined to their original territories. LECs undergo apolysis, detach from the old larval cuticle and secrete the pupal cuticle. Images show the increment in number and the reduction in size of histoblasts from a ventral nest during pupariation. Histoblasts express GFP under the control of the *Esg-Gal4* driver. The cell cytoplasm is marked in red with Propidium Iodide. In pupal stages, histoblasts undertake stochastic cell divisions and nests expand to replace LECs. These extrude from the epithelia, die and are cleared by the action of circulating haemocytes. In the images, histoblasts and LECs can be distinguished by their size (nuclear DAPI staining). Images show in false colour the spreading of nests in the period between 18 and 30 hours APF. Colour coding is as in Fig. 1 (i.e. green, anterior dorsal; red, posterior dorsal; yellow, spiracular; blue, ventral nest). The proliferation and expansion of histoblasts and the death of LECs are very precisely triggered by external (hormonal) inputs. An early Ecdysone peak of expression activates the synchronous divisions of histoblasts in prepupae. A late peak of Ecdysone correlates with histoblast proliferation and LEC death are also in place. LECs do not die in the absence of histoblast proliferation; conversely, histoblasts do not expand when LEC death is blocked. Mutual exchange of distinct signals thus appears to be necessary, beyond hormonal triggering events, to implement and harmonize the behaviour of histoblasts and LECs during abdominal epithelial morphogenesis

although being considerably slower, the actin tails employed by *Listeria* to propel through the cytoplasm of infected cells (Skoble et al., 2001), or the actin-rich pseudopodia extended by neutrophils in response to chemoattractants (Weiner et al., 1999). Proper actin cytoskeleton dynamics appear to be essential to build up these protrusions and the full repertoire of activities leading to the expansion of histoblast nests. The equilibrium between actin polymerization and depolymerization activities should be exquisitely regulated, and the forced polymerization of actin by Profilin overexpression not only blocks the cytoskeletal dynamics of single cells, but impedes the spreading of the whole histoblast nest (Fig. 3). Potential roles for further actin dynamics regulators, the Arp2-Arp3 (Arp14D-Arp66B – FlyBase) complex, Dynamin (Shibire – FlyBase), membrane polyphosphoinositides, Cdc42, WASp-family proteins and other molecules (reviewed by Machesky, 1999) in building up these projections remain to be explored. Further, although these protrusions appear to have a mechanical role, they also seem to be involved in the recognition of guidance cues, as they follow stereotyped paths. Indeed, gradients of cell affinity have been described for the patterning of the *Drosophila* abdomen (Lawrence et al., 1999), and it would be of major interest to understand how these cells interpret the larval landscape.

The mechanism of LEC extrusion

The mechanisms involved in the death of LECs have been a matter of debate. While ultrastructural analysis suggests that LECs are phagocytosed (Roseland and Reinhardt, 1982), other studies suggested that LECs are histolyzed and die by autophagy (Juhász and Sass, 2005). Our findings are conclusive in this respect. The death of LECs involves a caspase-mediated apoptotic process that implicates cytoskeletal remodelling and apical cellular constriction leading to delamination. The actomyosin mediated contractile force of dying LECs contributes in bringing together neighbouring histoblasts. Once the LECs initiate extrusion, they become immediate targets for circulating haemocytes, which extend membrane projections and engulf them. Finally, LECs are degraded inside haemocytes (Figs 4 and 5).

Apical constriction is a process shared by multiple morphogenetic events, e.g. *Drosophila* mesodermal cells accumulate myosin and apically constrict during gastrulation under the control of the small GTPase Rho (Nikolaidou and Barrett, 2004). Myosin activity is also sufficient to promote the apical constriction and elimination of photoreceptor cells in the *Drosophila* eye in response to the overexpression of an activated form of the Rok kinase (Rosenblatt

et al., 2001). Indeed, we found that the apical contractility of LECs depends on the level of phosphorylation of the MRLC and could be enhanced or abolished by modulating the counteracting kinase and phosphatase activities of Rok and MLCP (Fig. 4). As a consequence, LEC delamination is either accelerated or delayed. How these regulatory activities are themselves regulated remains to be established. Yet, the LEC extrusion defects observed in weakened caspase cascade conditions after P35 overexpression (Fig. 7B,C) strongly suggest that apoptotic signals could be involved in the trigger of actomyosin contractility in LECs. Apical contraction would thus be an early event in the LEC apoptotic process. Being particularly important to analyse the differences that modulate the activity of myosin during apical constriction of living cells and during extrusion of apoptotic cells, the replacement of LECs could become an exceptionally suitable model to unravel how myosin activity is regulated in apoptotic cells in vivo.

The recruitment of haemocytes to dying LECs during abdominal cell replacement is extremely fast. The apical constriction of LECs takes about 2 hours, but the time that a haemocyte needs to fully engulf a LEC is less than 10 minutes. This entails a very reliable chemoattracting mechanism. In mammals, caspase 3-dependent lipid attraction signals, released by dying cells, induce the migration of phagocytes (Lauber et al., 2003). Furthermore, several receptors are implicated in corpse recognition, including lectins, integrins, tyrosine kinases, the phosphatidylserine receptor (PSR) and scavenger receptors (Krieser and White, 2002). In *Drosophila*, the elements involved in cell recognition by macrophages are mostly unknown. Haemocytes express Croquemort, a scavenger receptor homologue, which is required for the uptake of dead cells (Franc et al., 1999), and Pvr, a homologue of the vertebrate PDGF/VEGF receptor that seems to affect their motility (Cho et al., 2002). Still, the signals that haemocytes recognize in dying cells and the links between those signals and the apoptotic cascade are essentially unknown.

As macrophages are responsible for much of the engulfment of dead cells in developing animals, an important role for macrophages in tissue morphogenesis has been suggested (Sears et al., 2003). However, this is not the case during abdominal morphogenesis, as the inhibition of haemocyte motility, which abrogates the removal of LECs, does not affect their replacement by histoblasts. Our results are consistent with studies showing that macrophage removal of cell debris is not required for the regeneration of laser-induced wounds in *Drosophila* (Stramer et al., 2005).

Cell cooperation or cell competition in epithelial cell replacement

Histoblast nest expansion is tightly coordinated with LEC removal. A naive view of the process of LEC extrusion suggests that their death is altruistic – it would promote the expansion of histoblasts. However, several results suggest that LECs do not execute this process autonomously. First, histoblast nests initiate their expansion in the absence of LEC death. Second, histoblast nests, during their spreading, grow, with no obvious planar orientation, by stochastic cell divisions not restricted to their edges (Fig. 1). Finally, and most importantly, the inhibition of histoblast proliferation exerts non-autonomous effects on both extrusion and removal of LECs (Fig. 7). A working model in which histoblast proliferation and LEC death are synchronized by a spatially and temporally controlled exchange of signals (secreted ligands or cell-to-cell communication modules) is thus strongly appealing. This potential mechanism for replacement of LECs by histoblasts somewhat resembles the elimination and death by anoikis of amnioserosa cells upon dorsal

closure completion during *Drosophila* embryogenesis (Reed et al., 2004). Through this process, physical contacts and intracellular signalling among epithelial leading cells, the amnioserosa and the yolk sac coordinate the different behaviour of these cell types, which is essential for the accurate progress of both germ band retraction and dorsal closure. In this scenario, coordinated extrinsic and intrinsic events, hormonal inputs, cell contacts and cell signalling events will be responsible for the ordered proliferation and expansion of histoblasts and the extrusion and death of LECs.

An alternative mechanism for the ordered cell substitution taking place during abdominal morphogenesis involving cell competition could also be proposed. Competition can be defined as an interaction between individuals brought about by a shared requirement leading to a reduction in the survivorship, growth and/or reproduction rates. Classical experiments in *Drosophila* imaginal discs have shown that cells heterozygous mutant for ribosomal protein genes (*Minutes*) placed beside wild-type cells are outcompeted and eliminated from the epithelium (Morata and Ripoll, 1975). More recent work has shown that imaginal wild-type cells are outcompeted by cells with growth advantage overexpressing the proto-oncogene *Myc* (Moreno and Basler, 2004). Cell competition does not just apply to the fight for survival of cells with their ‘fitness’ experimentally altered, but also applies to the homeostasis of self-renewing cell pools such as lymphocytes (Gett et al., 2003) or stem cells (Oertel et al., 2006). The substitution of LECs by histoblasts closely resembles cell competition. Rapidly dividing and expanding histoblasts may become competent to displace the surrounding less-metabolically-active LECs. During normal development, having ‘weaker’ neighbours, histoblasts do not compete against each other, and cells from *Minute* clones in the abdomen are not eliminated in heterozygous animals (Morata and Ripoll, 1975). However, when confronted with death-resistant LECs (Fig. 7), ‘winner’ histoblasts may become ‘losers’. Histoblasts in an increasingly crowded environment will compete against each other, and the less fit individuals (less competent in signalling reception and transduction, or with slower proliferation rates) would eventually become more sensitive to ‘killing’ signals and would die.

Our findings here demonstrate that the replacement of LECs by histoblasts, independently of being driven by cooperative mechanisms, cell competition or both, represents an extremely amenable morphogenetic model for the study of the dynamic control of the cell cycle and cell death, of the coordination of cytoskeleton activities and cell adhesion, and for the study of cell invasiveness.

Supplementary material

Supplementary material for this article is available at <http://dev.biologists.org/cgi/content/full/134/2/367/DC1>

The authors would like to acknowledge the different groups that have provided reagents and fly stocks to perform this work, in particular C. Antoniewski, S. Baumgartner, A. Brand, L. Cooley, S. Hayashi, E. Knust, C. Lehner, E. Marti, E. Rebollo, P. Rorth, D. Strutt and J. Treisman. We also want to thank C. Thummel, T. Kornberg and D. Shaye and members of the laboratory for their encouragement and for taking the time to look at and comment on the manuscript. Special thanks to Antonio LoNigro, who helped in some critical aspects of this project. NN was supported by a PhD Studentship of FPU programme of the Spanish Ministerio de Educación y Ciencia. This work was funded by grants of the DGICYT (Spanish Ministerio de Educación y Ciencia) and a STREP project (WOUND-LSHG-CT-2003-503447) of the European Union.

References

- Bard, J. (1990). *Morphogenesis: The Cellular and Molecular Basis of Developmental Anatomy*. Cambridge, New York: Cambridge University Press.
Bender, M., Imam, F. B., Talbot, W. S., Ganetzky, B. and Hogness, D. S.

- (1997). Drosophila ecdysone receptor mutations reveal functional differences among receptor isoforms. *Cell* **91**, 777-788.
- Bershadsky, A.** (2004). Magic touch: how does cell-cell adhesion trigger actin assembly? *Trends Cell Biol.* **14**, 589-593.
- Brand, A. H.** (1995). GFP in Drosophila. *Trends Genet.* **11**, 324-325.
- Brand, A. H. and Perrimon, N.** (1993). Targeted gene expression as a means of altering cell fates and generating dominant phenotypes. *Development* **118**, 401-415.
- Bruckner, K., Kockel, L., Duchek, P., Luque, C. M., Rorth, P. and Perrimon, N.** (2004). The PDGF/VEGF receptor controls blood cell survival in Drosophila. *Dev. Cell* **7**, 73-84.
- Champlin, D. T. and Truman, J. W.** (1998). Ecdysteroid control of cell proliferation during optic lobe neurogenesis in the moth *Manduca sexta*. *Development* **125**, 269-277.
- Cherbas, L., Hu, X., Zhimulev, I., Belyaeva, E. and Cherbas, P.** (2003). EcR isoforms in Drosophila: testing tissue-specific requirements by targeted blockade and rescue. *Development* **130**, 271-284.
- Cho, N. K., Keyes, L., Johnson, E., Heller, J., Ryner, L., Karim, F. and Krasnow, M. A.** (2002). Developmental control of blood cell migration by the Drosophila VEGF pathway. *Cell* **108**, 865-876.
- Craig, R., Smith, R. and Kendrick-Jones, J.** (1983). Light-chain phosphorylation controls the conformation of vertebrate non-muscle and smooth muscle myosin molecules. *Nature* **302**, 436-439.
- de Nooij, J. C., Letendre, M. A. and Hariharan, I. K.** (1996). A cyclin-dependent kinase inhibitor, Dacapo, is necessary for timely exit from the cell cycle during Drosophila embryogenesis. *Cell* **87**, 1237-1247.
- Fessler, L. I., Campbell, A. G., Duncan, K. G. and Fessler, J. H.** (1987). Drosophila laminin: characterization and localization. *J. Cell Biol.* **105**, 2383-2391.
- Franc, N. C., Heitzler, P., Ezekowitz, R. A. and White, K.** (1999). Requirement for croquemort in phagocytosis of apoptotic cells in Drosophila. *Science* **284**, 1991-1994.
- Fukata, Y., Kimura, K., Oshiro, N., Saya, H., Matsuura, Y. and Kaibuchi, K.** (1998). Association of the myosin-binding subunit of myosin phosphatase and moesin: dual regulation of moesin phosphorylation by Rho-associated kinase and myosin phosphatase. *J. Cell Biol.* **141**, 409-418.
- Garcia-Bellido, A. and Merriam, J. R.** (1971). Clonal parameters of tergite development in Drosophila. *Dev. Biol.* **26**, 264-276.
- Gett, A. V., Sallusto, F., Lanzavecchia, A. and Geginat, J.** (2003). T cell fitness determined by signal strength. *Nat. Immunol.* **4**, 355-360.
- Guerra, M., Postlethwait, J. H. and Schneiderman, H. A.** (1973). The development of the imaginal abdomen of *Drosophila melanogaster*. *Dev. Biol.* **32**, 361-372.
- Harden, N.** (2002). Signaling pathways directing the movement and fusion of epithelial sheets: lessons from dorsal closure in Drosophila. *Differentiation* **70**, 181-203.
- Hopmann, R. and Miller, K. G.** (2003). A balance of capping protein and profilin functions is required to regulate actin polymerization in Drosophila bristle. *Mol. Biol. Cell* **14**, 118-128.
- Ito, K., Awano, W., Suzuki, K., Hiromi, Y. and Yamamoto, D.** (1997). The Drosophila mushroom body is a quadruple structure of clonal units each of which contains a virtually identical set of neurones and glial cells. *Development* **124**, 761-771.
- Jiang, C., Lamblin, A. F., Steller, H. and Thummel, C. S.** (2000). A steroid-triggered transcriptional hierarchy controls salivary gland cell death during Drosophila metamorphosis. *Mol. Cell* **5**, 445-455.
- Jorgensen, P. and Tyers, M.** (2004). How cells coordinate growth and division. *Curr. Biol.* **14**, R1014-R1027.
- Juhász, G. and Sass, M.** (2005). Hid can induce, but is not required for autophagy in polyploid larval Drosophila tissues. *Eur. J. Cell Biol.* **84**, 491-502.
- Kawano, Y., Fukata, Y., Oshiro, N., Amano, M., Nakamura, T., Ito, M., Matsumura, F., Inagaki, M. and Kaibuchi, K.** (1999). Phosphorylation of myosin-binding subunit (MBS) of myosin phosphatase by Rho-kinase in vivo. *J. Cell Biol.* **147**, 1023-1038.
- Keller, R., Davidson, L., Edlund, A., Elul, T., Ezin, M., Shook, D. and Skoglund, P.** (2000). Mechanisms of convergence and extension by cell intercalation. *Philos. Trans. R. Soc. Lond. B Biol. Sci.* **355**, 897-922.
- Knoblich, J. A., Sauer, K., Jones, L., Richardson, H., Saint, R. and Lehner, C. F.** (1994). Cyclin E controls S phase progression and its down-regulation during Drosophila embryogenesis is required for the arrest of cell proliferation. *Cell* **77**, 107-120.
- Kockel, L., Zeitlinger, J., Staszewski, L. M., Mlodzik, M. and Bohmann, D.** (1997). Jun in Drosophila development: redundant and nonredundant functions and regulation by two MAPK signal transduction pathways. *Genes Dev.* **11**, 1748-1758.
- Koelle, M. R., Talbot, W. S., Segraves, W. A., Bender, M. T., Cherbas, P. and Hogness, D. S.** (1991). The Drosophila EcR gene encodes an ecdysone receptor, a new member of the steroid receptor superfamily. *Cell* **67**, 59-77.
- Korn, E. D. and Hammer, J. A.** (1988). Myosins of nonmuscle cells. *Annu. Rev. Biophys. Chem.* **17**, 23-45.
- Krieser, R. J. and White, K.** (2002). Engulfment mechanism of apoptotic cells. *Curr. Opin. Cell Biol.* **14**, 734-738.
- Lane, M. E., Sauer, K., Wallace, K., Jan, Y. N., Lehner, C. F. and Vaessin, H.** (1996). Dacapo, a cyclin-dependent kinase inhibitor, stops cell proliferation during Drosophila development. *Cell* **87**, 1225-1235.
- Lauber, K., Bohn, E., Krober, S. M., Xiao, Y. J., Blumenthal, S. G., Lindemann, R. K., Marini, P., Wiedig, C., Zobywalski, A., Baksh, S. et al.** (2003). Apoptotic cells induce migration of phagocytes via caspase-3-mediated release of a lipid attraction signal. *Cell* **113**, 717-730.
- Lawrence, P. A., Casal, J. and Struhl, G.** (1999). The hedgehog morphogen and gradients of cell affinity in the abdomen of Drosophila. *Development* **126**, 2441-2449.
- Lee, A. and Treisman, J. E.** (2004). Excessive Myosin activity in mbs mutants causes photoreceptor movement out of the Drosophila eye disc epithelium. *Mol. Biol. Cell* **15**, 3285-3295.
- Lee, C. Y., Cooksey, B. A. and Baehrecke, E. H.** (2002). Steroid regulation of midgut cell death during Drosophila development. *Dev. Biol.* **250**, 101-111.
- Machesky, L. M.** (1999). Rocket-based motility: a universal mechanism? *Nat. Cell Biol.* **1**, E29-E31.
- Madhavan, M. M. and Schneiderman, H. A.** (1977). Histological analysis of the dynamics of growth of imaginal discs and histoblast nests during the larval development of *Drosophila melanogaster*. *Dev. Genes Evol.* **183**, 269-305.
- Madhavan, M. M. and Madhavan, K.** (1980). Morphogenesis of the epidermis of adult abdomen of Drosophila. *J. Embryol. Exp. Morphol.* **60**, 1-31.
- Martin, P. and Wood, W.** (2002). Epithelial fusions in the embryo. *Curr. Opin. Cell Biol.* **14**, 569-574.
- Martin-Blanco, E. and Knust, E.** (2001). Epithelial morphogenesis: filopodia at work. *Curr. Biol.* **11**, R28-R31.
- Martin-Blanco, E., Gampel, A., Ring, J., Virdee, K., Kirov, N., Tolkovsky, A. M. and Martinez-Arias, A.** (1998). puckered encodes a phosphatase that mediates a feedback loop regulating JNK activity during dorsal closure in Drosophila. *Genes Dev.* **12**, 557-570.
- Merriam, J. R.** (1978). Estimating primordial cell numbers in Drosophila imaginal discs and histoblasts. *Results Probl. Cell Differ.* **9**, 71-96.
- Milner, M. J.** (1977). The eversion and differentiation of Drosophila melanogaster leg and wing imaginal discs cultured in vitro with an optimal concentration of beta-ecdysone. *J. Embryol. Exp. Morphol.* **37**, 105-117.
- Morata, G. and Ripoll, P.** (1975). Minutes: mutants of Drosophila autonomously affecting cell division rate. *Dev. Biol.* **42**, 211-221.
- Moreno, E. and Basler, K.** (2004). dMyc transforms cells into super-competitors. *Cell* **117**, 117-129.
- Nikolaïdou, K. K. and Barrett, K.** (2004). A Rho GTPase signaling pathway is used iteratively in epithelial folding and potentially selects the outcome of Rho activation. *Curr. Biol.* **14**, 1822-1826.
- Oda, H. and Tsukita, S.** (2001). Real-time imaging of cell-cell adherens junctions reveals that Drosophila mesoderm invagination begins with two phases of apical constriction of cells. *J. Cell Sci.* **114**, 493-501.
- Oertel, M., Menthen, A., Dabeva, M. D. and Shafritz, D. A.** (2006). Cell competition leads to a high level of normal liver reconstitution by transplanted fetal liver stem/progenitor cells. *Gastroenterology* **130**, 507-520.
- Paladi, M. and Tepass, U.** (2004). Function of Rho GTPases in embryonic blood cell migration in Drosophila. *J. Cell Sci.* **117**, 6313-6326.
- Pastor-Pareja, J. C., Grawe, F., Martin-Blanco, E. and Garcia-Bellido, A.** (2004). Invasive cell behavior during Drosophila imaginal disc eversion is mediated by the JNK signaling cascade. *Dev. Cell* **7**, 387-399.
- Rebollo, E., Llamazares, S., Reina, J. and Gonzalez, C.** (2004). Contribution of noncentrosomal microtubules to spindle assembly in Drosophila spermatocytes. *PLoS Biol.* **2**, 54-64.
- Reed, B. H., Wilk, R., Schock, F. and Lipshitz, H. D.** (2004). Integrin-dependent apposition of Drosophila extraembryonic membranes promotes morphogenesis and prevents anokis. *Curr. Biol.* **14**, 372-380.
- Riddiford, L. M.** (1993). Hormone receptors and the regulation of insect metamorphosis. *Receptor* **3**, 203-209.
- Riesgo-Escovar, J. R. and Hafen, E.** (1997). Drosophila Jun kinase regulates expression of decapentaplegic via the ETS-domain protein Aop and the AP-1 transcription factor DJun during dorsal closure. *Genes Dev.* **11**, 1717-1727.
- Roseland, C. R. and Reinhardt, C.** (1982). Abdominal development. In *A Handbook of Drosophila Development* (ed. R. Ransom), pp. 215-235. Amsterdam: Elsevier.
- Roseland, C. R. and Schneiderman, H. A.** (1979). Regulation and metamorphosis of the abdominal histoblasts of *Drosophila melanogaster*. *Dev. Genes Evol.* **186**, 235-265.
- Rosenblatt, J., Raff, M. C. and Cramer, L. P.** (2001). An epithelial cell destined for apoptosis signals its neighbors to extrude it by an actin- and myosin-dependent mechanism. *Curr. Biol.* **11**, 1847-1857.
- Rouyou, A., Field, C., Sisson, J. C., Sullivan, W. and Kares, R.** (2004). Reassessing the role and dynamics of nonmuscle myosin II during furrow formation in early Drosophila embryos. *Mol. Biol. Cell* **15**, 838-850.
- Schubiger, M., Wade, A. A., Carney, G. E., Truman, J. W. and Bender, M.**

- (1998). *Drosophila* EcR-B ecdysone receptor isoforms are required for larval molting and for neuron remodeling during metamorphosis. *Development* **125**, 2053-2062.
- Schubiger, M., Carre, C., Antoniewski, C. and Truman, J. W.** (2005). Ligand-dependent de-repression via EcR/USP acts as a gate to coordinate the differentiation of sensory neurons in the *Drosophila* wing. *Development* **132**, 5239-5248.
- Sears, H. C., Kennedy, C. J. and Garrity, P. A.** (2003). Macrophage-mediated corpse engulfment is required for normal *Drosophila* CNS morphogenesis. *Development* **130**, 3557-3565.
- Skoble, J., Auerbuch, V., Goley, E. D., Welch, M. D. and Portnoy, D. A.** (2001). Pivotal role of VASP in Arp2/3 complex-mediated actin nucleation, actin branch-formation, and *Listeria monocytogenes* motility. *J. Cell Biol.* **155**, 89-100.
- Stramer, B., Wood, W., Galko, M. J., Redd, M. J., Jacinto, A., Parkhurst, S. M. and Martin, P.** (2005). Live imaging of wound inflammation in *Drosophila* embryos reveals key roles for small GTPases during *in vivo* cell migration. *J. Cell Biol.* **168**, 567-573.
- Struhl, G. and Basler, K.** (1993). Organizing activity of wingless protein in *Drosophila*. *Cell* **72**, 527-540.
- Strutt, D., Johnson, R., Cooper, K. and Bray, S.** (2002). Asymmetric localization of frizzled and the determination of notch-dependent cell fate in the *Drosophila* eye. *Curr. Biol.* **12**, 813-824.
- Talbot, W. S., Swyryd, E. A. and Hogness, D. S.** (1993). *Drosophila* tissues with different metamorphic responses to ecdysone express different ecdysone receptor isoforms. *Cell* **73**, 1323-1337.
- Tepass, U., Fessler, L. I., Aziz, A. and Hartenstein, V.** (1994). Embryonic origin of hemocytes and their relationship to cell death in *Drosophila*. *Development* **120**, 1829-1837.
- Thummel, C. S.** (2001). Molecular mechanisms of developmental timing in *C. elegans* and *Drosophila*. *Dev. Cell* **1**, 453-465.
- Thummel, C. S.** (2002). Ecdysone-regulated puff genes 2000. *Insect Biochem. Mol. Biol.* **32**, 113-120.
- Totsukawa, G., Yamakita, Y., Yamashiro, S., Hartshorne, D. J., Sasaki, Y. and Matsumura, F.** (2000). Distinct roles of ROCK (Rho-kinase) and MLCK in spatial regulation of MLC phosphorylation for assembly of stress fibers and focal adhesions in 3T3 fibroblasts. *J. Cell Biol.* **150**, 797-806.
- Trinkaus, J. P., Trinkaus, M. and Fink, R. D.** (1992). On the convergent cell movements of gastrulation in *Fundulus*. *J. Exp. Zool.* **261**, 40-61.
- Wang, P., Hayden, S. and Masui, Y.** (2000). Transition of the blastomere cell cycle from cell size-independent to size-dependent control at the midblastula stage in *Xenopus laevis*. *J. Exp. Zool.* **287**, 128-144.
- Weiner, O. D., Servant, G., Welch, M. D., Mitchison, T. J., Sedat, J. W. and Bourne, H. R.** (1999). Spatial control of actin polymerization during neutrophil chemotaxis. *Nat. Cell Biol.* **1**, 75-81.
- Williams-Masson, E. M., Malik, A. N. and Hardin, J.** (1997). An actin-mediated two-step mechanism is required for ventral enclosure of the *C. elegans* hypodermis. *Development* **124**, 2889-2901.
- Winter, C. G., Wang, B., Ballew, A., Royou, A., Kares, R., Axelrod, J. D. and Luo, L.** (2001). *Drosophila* Rho-associated kinase (Drok) links Frizzled-mediated planar cell polarity signaling to the actin cytoskeleton. *Cell* **105**, 81-91.
- Yao, T. P., Segraves, W. A., Oro, A. E., McKeown, M. and Evans, R. M.** (1992). *Drosophila* ultraspiracle modulates ecdysone receptor function via heterodimer formation. *Cell* **71**, 63-72.